Circulation Journal
Circ J 2021; 85: 677–686
doi:10.1253/circj.CJ-20-1008

ORIGINAL ARTICLE
Cardiomyopathy

Cardiac Fibroblasts Play Pathogenic Roles in Idiopathic Restrictive Cardiomyopathy

Hirofumi Tsuru, MD; Hidekazu Ishida, MD, PhD; Jun Narita, MD; Ryo Ishii, MD; Hidehiro Suginobe, MD; Yoichiro Ishii, MD; Renjie Wang; Shigetoyo Kogaki, MD; Masaki Taira, MD; Takayoshi Ueno, MD, PhD; Yohei Miyashita, MD, PhD; Hidetaka Kioka, MD, PhD; Yoshihiro Asano, MD, PhD; Yoshiki Sawa, MD, PhD; Keiichi Ozono, MD, PhD

Background: Restrictive cardiomyopathy (RCM) is characterized by impaired ventricular relaxation. Although several mutations were reported in some patients, no mutations were identified in cardiomyocyte expressing genes of other patients, indicating that pathological mechanisms underlying RCM could not be determined by cardiomyocytes only. Cardiac fibroblasts (CFs) are a major cell population in the heart; however, the pathological roles of CFs in cardiomyopathy are not fully understood.

Methods and Results: This study established 4 primary culture lines of CFs from RCM patients and analyzed their cellular physiology, the effects on the contraction and relaxation ability of healthy cardiomyocytes under co-culture with CFs, and RNA sequencing. Three of four patients had *TNNI3* mutations. There were no significant alterations in cell proliferation, apoptosis, migration, activation, and attachment. However, when CFs from RCM patients were co-cultured with healthy cardiomyocytes, the relaxation velocity of cardiomyocytes was significantly impaired both under direct and indirect co-culture conditions. RNA sequencing revealed that gene expression profiles of CFs in RCM were clearly distinct from healthy CFs. The differential expression gene analysis identified that several extracellular matrix components and cytokine expressions were dysregulated in CFs from RCM patients.

Conclusions: The comprehensive gene expression patterns were altered in RCM-derived CFs, which deteriorated the relaxation ability of cardiomyocytes. The specific changes in extracellular matrix composition and cytokine secretion from CFs might affect pathological behavior of cardiomyocytes in RCM.

Key Words: Cardiac fibroblast; Cardiomyocyte; Motion analysis; Restrictive cardiomyopathy; RNA seq

Restrictive cardiomyopathy (RCM) is characterized by impaired diastolic function with preserved ventricular systolic function and wall thickness. Congestion due to increased ventricular end diastolic pressure causes clinical symptoms; however, no medical therapy has been established to treat diastolic dysfunction. The prognosis of young children with RCM is terribly poor, and heart transplantation is the only method for treatment.[1,2] The pathogenesis of cardiomyopathy varies, and to date, numerous causes of RCM have been investigated. The histology of the myocardium in RCM patients is usually non-specific, with mild myocyte hypertrophy and disarray, as well as slight interstitial fibrosis. Recently, multiple studies, including those using whole exome sequencing, have identified several causative genes, such as *MYH7*, *TNNT2*, and *TNNI3*.[3–5] Several previous studies elucidated that these mutants could alter myofilament calcium sensitivity and dissociation.[6–8] However, disease-causing gene variants were only found in 25–50% of RCM patients, despite vigorous gene analyses.[3,9] Moreover, different mutations in these genes can contribute to similar phenotype; however, the same mutations in these genes may also cause different phenotypes of cardiomyopathy.[4,9,10] The relationship between genotype and phenotype is thought to be limited in cardiomyopathy, and not all etiologies of cardiomyopathy could be explained by gene mutations in cardiomyocytes. Cardiomyocytes are not the only cell type constituting the

Editorial p 687

Received September 30, 2020; revised manuscript received December 8, 2020; accepted December 10, 2020; J-STAGE Advance Publication released online February 13, 2021 Time for primary review: 16 days

Department of Pediatrics (H.T., H.I., J.N., R.I., H.S., R.W., S.K., K.O.), Department of Cardiovascular Surgery (M.T., T.U., Y.S.), Department of Cardiology (Y.M., H.K., Y.A.), Osaka University Graduate School of Medicine, Suita; Department of Pediatric Cardiology, Osaka Women's and Children's Hospital, Izumi (Y.I.); and Department of Pediatrics and Neonatology, Osaka General Medical Center, Osaka (S.K.), Japan

Mailing address: Hidekazu Ishida, MD, PhD, Department of Pediatrics, Osaka University Graduate School of Medicine, 2-2 Yamadaoka, Suita 565-0871, Japan. E-mail: hideishi@ped.med.osaka-u.ac.jp

ISSN-1346-9843

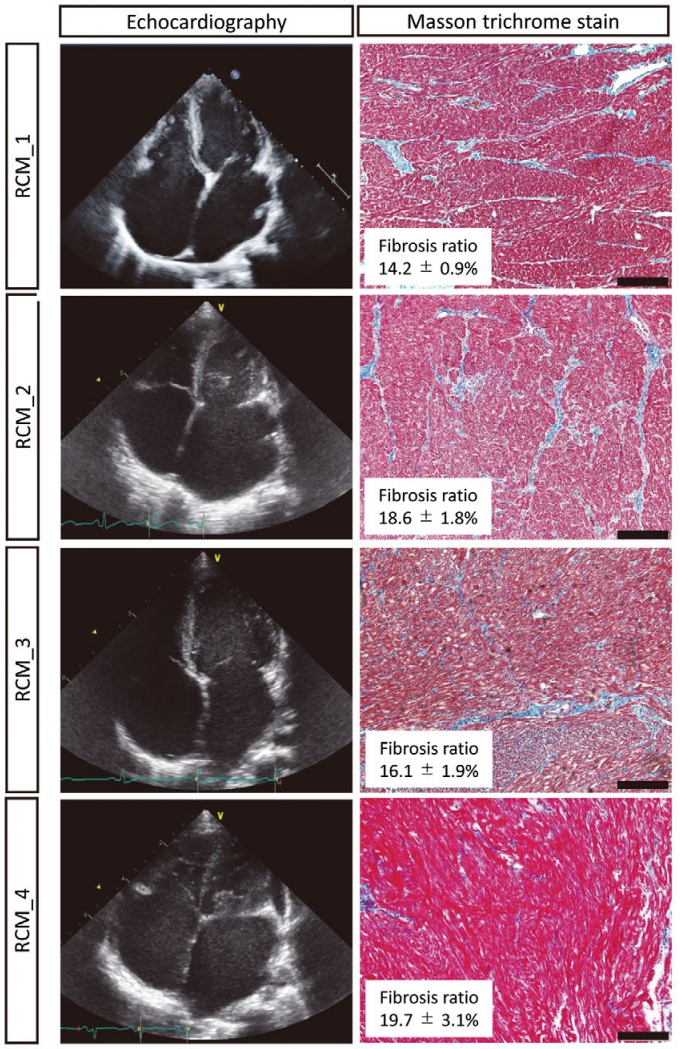

Figure 1. Clinical echocardiographic and histological data of the patients. Echocardiographic findings of each patient demonstrated massively dilated right and left atria with restrictive ventricular dysfunction. The Masson's trichrome stain utilized on cardiac tissue from all patients evidenced only mild interstitial fibrosis (blue stain). The fibrosis ratio was evaluated by using 5 different locations of the sections and was not significantly different among the patients. Scale bar: 200 μm.

human heart. In fact, cardiac fibroblasts (CFs) are the most abundant cells in the heart, accounting for 60% of cells in a normal heart. To date, various previous studies have demonstrated that CFs could affect cardiomyocyte behavior in response to chemical, electrical, and mechanical stimuli, suggesting that CFs play pivotal roles in maintaining cardiac function under healthy conditions and diseased statuses.[11–13] These reports and experiments have been conducted using animal models mimicking myocardial infarction and hypertensive cardiac diseases. However, the pathogenic roles of CFs in idiopathic cardiomyopathy, especially in RCM, remain unclear. In this study, we investigated the physiological and transcriptional features of human CFs obtained from pure RCM pediatric patients. Additionally, we co-cultured patient-derived CFs with normal cardiomyocytes to evaluate the interaction between them.

Methods

Ethical Statement

We obtained written informed consent from the parents of the minors included in this study. This research project (no. 15211 and no. 442) was approved by the Osaka University Clinical Research Review Committee.

Fibrosis Ratio

The fibrosis ratio of each patient's specimen was calculated by using ImageJ software (https://imagej.nih.gov/ij/) with Masson trichrome staining of the heart tissue sections. Five different locations were measured and the data were shown as mean±standard error (**Figure 1**).

Cell Culture

CFs were harvested from the heart tissues, which were obtained during heart transplantation or ventricular assist device implantation. The left ventricular tissues were minced, seeded onto cell culture dishes, and incubated in Dulbecco's modified Eagle's medium (DMEM) with 10% fetal bovine serum (FBS) and 1% penicillin/streptomycin (P/S). The majority of adherent cells were considered as CFs, assessed by morphological observation and immunocytochemistry of von Willbrand Factor (vWF) and smooth muscle myosin heavy chain (SM-MHC) (**Supplementary Figure 1**). Cell culture was achieved in a humidified incubator with media exchange every 2–3 days. Three samples of healthy CFs were purchased from PromoCell (13-year-old

(y.o.) male, 25 y.o. female, and 30 y.o. female; all Caucasian), and were cultured using the same procedure described above. Cells between passage number 4 and 7 were used for all experiments.

Proliferation Assay

Cells were seeded at 5×10^3 cells per well into 96-well plates and incubated in DMEM/10% FBS overnight. Thereafter, 10 μmol/L EdU was added and incubated for 24 h according to the manufacturer's instructions.[14] The EdU-positive nuclei were analyzed by the In Cell Analyzer 6000 using Click-iT® EdU Imaging Kits. Independent three experiments were conducted for the assay.

Apoptosis and Myofibroblast Assay

Cells were seeded at 5×10^3 cells per well into 96-well plates and incubated in DMEM/10% FBS for 24 h, and then incubated for another 48 h under the following 4 conditions: (1) DMEM with FBS in a normoxic environment; (2) serum-deficient DMEM in a normoxic environment; (3) DMEM with FBS in a hypoxic environment (1% O_2); and (4) serum-deficient DMEM in a hypoxic environment (1% O_2). Samples were reacted overnight at 4°C with cleaved caspase-3 and α-SMA antibodies (1 : 500; purchased from Cell Signaling: catalog no. 9661, and Invitrogen: catalog no.14-9760-82). After incubating with secondary antibodies, Alexa594 and Alexa488 (1 : 500; Invitrogen), at room temperature for 30 min, nuclei were dyed with Hoechst33342 (1 : 1,000; Dojindo). The percentage of cleaved caspase-3-positive cells and cytoplasmic α-SMA-positive cells were analyzed using the In Cell Analyzer 6000. Independent three experiments were conducted for each assay.

Migration Assay

Cells were seeded at 3×10^4 cells per well into 96-well plates 24 h prior to assay. After confirming confluence, cell monolayers were scratched using a 10 μL pipette tip and a vertical wound was created. Phase contrast microscopic images were saved and the distance from one side of the wound to the other was measured. The ratio of shortening from start to 12-h post-scratching was analyzed using ImageJ software.[15] Independent three experiments were conducted for the assay.

Attachment Assay

Cells were seeded at 5×10^3 cells per well into 96-well plates; thereafter, the medium was removed and cells were gently washed with phosphate-buffered saline (PBS) 4 h after seeding. Nuclei were stained with Hoechst33342 and the number of attached cells were counted using the In Cell Analyzer (sum of cells of 20 fields per well). Independent three experiments were conducted for the assay.

Primary Culture of Rat Cardiomyocytes

Two-day-old Sprague-Dawley rats were used in experiments after approval was obtained from the Institutional Review Board of Osaka University. Cardiomyocytes were obtained using a previously described procedure with modifications.[16] Briefly, the ventricular tissues were isolated and minced, thereafter the tissue fragments were processed with collagenase and trypsin for 2 min in a 37°C water bath and filtered. The above process was repeated 7–8 times after which the cells obtained were seeded on cell culture plates in DMEM supplemented with 10% FBS and 1% P/S. In order to remove cardiac non-myocytes for cardiomyocytes purification, non-adherent cells were collected 1 h after incubation using the pre-plating technique.[17]

Co-Culture of Human CFs and Rat Cardiomyocytes

For direct 2D co-cultures, CFs were seeded at 3×10^4 cells per well in 96-well plates coated with 1% gelatin 24 h before the start of co-culture. After confirming confluence of CFs, rat myocytes were added at 6×10^4 cells per well.

For indirect co-cultures, we used a 0.4-μm Transwell®-96well plate (Corning). CFs (1.5×10^4) were seeded onto an insert plate 24 h before the initiation of co-culture in order to obtain confluence. Rat cardiomyocytes were seeded at 6×10^4 cells per well into a 96-well plate coated with 1% gelatin and co-cultured with CFs in the upper chamber.[14] After 48 h of co-culture, we analyzed the function of rat cardiomyocytes by detecting cell motility and mRNA expressions. Four independent co-culture assays were conducted for each analysis.

Quantitative Real-Time Polymerase Chain Reaction (qPCR)

After 48 h of incubation, cells from co-cultures were harvested and the total RNA was extracted using the RNA column kit (Nucleospin). Reverse transcription was performed using ReverTra Ace (TOYOBO), followed by qPCR with the Light-Cycler 480 using the THUDERBIRD SYBR qPCR Mix kit (TOYOBO). The following primer pairs, which were specifically designed for rat mRNA, were used for qPCR.[18–20] Each sample was analyzed in technical triplicates using the following protocol: 10 min at 95°C, followed by 40 cycles of 15 s at 95°C, and then 1 min at 60°C. Each PCR analysis was completed by a melt curve cycle of 15 s at 95°C, 60 s at 60°C, and 15 s at 95°C. Data were analyzed using the standard curve method. At the end of each PCR run, the relative amount of *Nppa*, *Nppb*, *Myh7*, and *Cx43* mRNA, in comparison to the housekeeping gene, *Gapdh*, was evaluated as previously described.[19,21] The forward and reverse primers for *Atp2a2* were 5'-ATTGACATCCATCAAGTCTACAACTCTG-3' and 5'-ATCTCAGTATTGACTCCAGTCGCC-3', respectively. Those for *Pln* were 5'-AACTAAACAGTCTG CATTGTGACGA-3' and 5'-GCCGAGCGAGTAAGG TATTGGA-3', respectively. Cycle threshold was calculated, under the default settings, by real-time sequence detection software (Applied Biosystems).

Motion Analysis of Cardiomyocytes

To evaluate the contractile and relaxation function of cardiomyocytes, we used the SI8000 Cell Motion Imaging System® (SONY). This system enables the quantitative analysis of the motion vector of beating cardiomyocytes by capturing high-quality videos. Cell movement is converted into a motion vector and the motion velocity within each region of interest (ROI) is calculated based on the sum of the vector magnitudes. The maximum contraction and relaxation velocity are considered to correspond to the contractile and diastolic function of the cardiomyocytes. ROIs were set to surround the cardiomyocyte nuclei, and we analyzed contraction velocity, relaxation velocity, and beating rate.[22,23] In indirect co-cultures, 10–20 cells were counted in each patient in 1 experiment. All data were obtained from isolated cardiomyocytes only (excluding clusters of cardiomyocytes). In direct co-cultures, all cells whose motion could be detected were analyzed; cardiomyocytes are usually isolated from other cardiomyocytes but were buried under layers of CFs. And 30–50 cells were

Table. Clinical Characteristics of the Patients

	RCM_1	RCM_2	RCM_3	RCM_4
Gender	Male	Male	Male	Female
Age at diagnosis (years)	5	2	6	8 months
Age at sampling (years)	10	3	11	2
Event at sampling	HTx	LVAD	LVAD	HTx
Medications at sampling	Dobutamine	Dobutamine	Milrinone	LVAD
	Milrinone	Milrinone	Diuretics	Dobutamine
	Diuretics	Diuretics	ACE inhibitor	Milrinone
	Amiodarone	β-blocker	Amiodarone	Diuretics
	Warfarin	Aspirin	Aspirin	Warfarin
BNP at sampling (pg/mL)	907.4	568.8	2,577.5	949.7
Gene mutation	*TNNI3* (K178E)	*TNNI3* (R170W)	*TNNI3* (R192H)	Not detected

ACE, angiotensin-converting enzyme; BNP, brain natriuretic peptide; HTx, heart transplantation; LVAD, left ventricular assist device; RCM, restrictive cardiomyopathy.

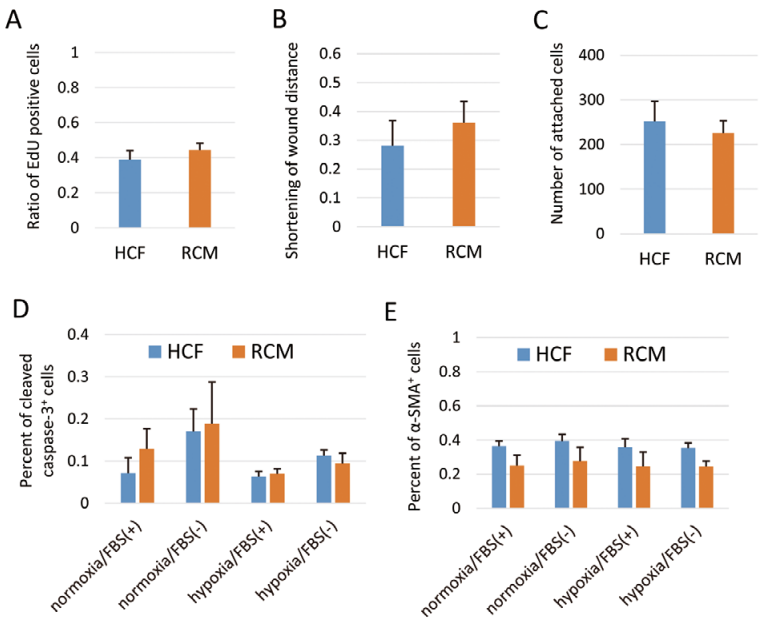

Figure 2. Cellular physiology assays of cardiac fibroblasts (CFs) derived from restrictive cardiomyopathy (RCM) patients. Three independent experiments were conducted for each patient for all experiments. The mean values and standard errors were calculated from 3 different lines of healthy CFs (HCF) and 4 different RCM patient-derived CFs. (**A**) A proliferation assay was performed to measure the number of EdU-positive cells. (**B**) A migration assay was performed by measuring the wound dimensions after scratching cell-culture dishes. (**C**) The result of the cell attachment assay, which evidenced no significant difference. (**D**) An apoptosis assay was performed to count the cleaved caspase-3-positive cells under a combination of hypoxia and serum starvation conditions. (**E**) A myofibroblast activation assay was performed to count the α-smooth muscle actin (SMA)-positive CFs under a combination of hypoxia and serum starvation conditions.

counted in each patient in 1 experiment. Four independent co-culture experiments were performed in each CF line from each patient.

Whole Exome Sequence Analysis

Genomic DNA was extracted from patients' peripheral blood samples using a DNeasy® Plant Mini Kit. The DNA was quantified using NanoDrop 2000c (Thermo Fisher Scientific). Genomic DNA was fragmented enzymatically or by ultrasonic irradiation. Fragmented DNA was hybridized with a biotin-labeled probe specific to the target region using SureSelect Human All Exon V6 kits (Agilent). Hybridized samples were enriched with streptavidin beads and captured DNA was amplified by on-bead PCR. Prepared genome libraries were sequenced as 100-bp paired-end runs on HiSeq 3000 systems (Illumina). Image analysis, base calling and demultiplexing were performed using the Illumina bcl2fastq2 conversion software v2.20. FASTQ files were quality checked using FASTQC and low-quality reads were removed using trimmomatic-0.36. Read alignment was performed using standard parameterized BWA v0.7.17 for human genome assembly hg19 (GRCh37). SNVs or short in/dels were called according to GATK best practice (GATK4.0.3). Called variants are filtered using GATK Variant Filtration, and variants that meet conditions of "QD <2.0, FS >60.0, MQ <40.0, MQRankSum <−12.5, ReadPosRankSum <−8.0, SQR >4.0" are analyzed.

Then, annotation information was added to the obtained variant list using Annovar. The narrowing down analysis from the mutation list was performed using the original script by Python3.6. The type of the variant and its position on the gene were determined from the annotation of UCSC Known Genes, RefSeq genes and Ensemble genes.

Candidate variants were present on the 257 gene associated with cardiomyopathy, and those with a minor allele frequency (MAF) <0.5% were extracted. Continuously, to assess the potential functional effects of variants, 4 bioinformatic algorithms were used: HGMD, Intervar, CADD,

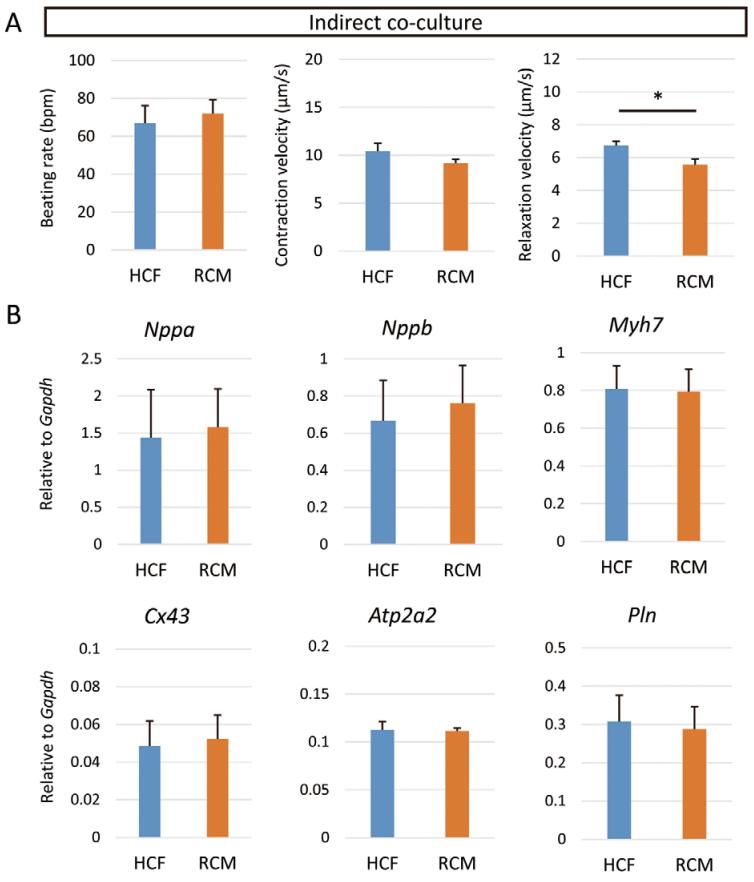

Figure 3. Indirect co-culture assays of patient-derived cardiac fibroblasts (CFs) and healthy rat cardiomyocytes. Three independent co-culture experiments were conducted for each patient. Ten to twenty beating cells were assayed in 1 experiment. The mean values were calculated from 3 different lines of healthy CFs (HCF) and 4 different restrictive cardiomyopathy (RCM) patient-derived CFs. The graphs show mean±standard error. (**A**) Motion analyses of healthy cardiomyocytes under indirect co-culture conditions with HCF and RCM CFs. (*P<0.05). (**B**) Quantitative real-time polymerase chain reaction (PCR) analyses of rat cardiomyocytes indirectly co-cultured with CFs. There was no significant difference between cardiomyocytes co-cultured with HCF and RCM CFs.

Protein variation effect analyzer (Provean). Missense variants were considered "potentially pathogenic" if classified simultaneously as "DM" by HGMD, "Pathogenic" or Likely pathogenic" by Intervar, CADD >25 and PROVEAN <2.5. These variants are infrequent and are considered to be highly pathogenic variants.

Comprehensive mRNA Expression Profiling of the CFs by Next Generation Sequencing

Total RNA was extracted from cultured CFs using a RNA column kit (Nucleospin) and evaluated by RNA sequencing using a next generation sequencer. Library preparation was performed using the TruSeq stranded mRNA sample prep kit (Illumina). An Illumina HiSeq 2500 platform in 75-base single-end mode was used for sequencing. Illumina CASAVA 1.8.2 software was used for base calling. Sequenced reads were mapped to the human reference genome sequence (hg19) using TopHat version 2.0.13 in combination with Bowtie2 version 2.2.3 and SAMtools version 0.1.19. Fragments per kilobase of exon per million mapped fragments were calculated using Cuffnorm version 2.2.1. Ingenuity Pathway Analysis was used to identify canonical pathways of differentially expressed genes. The transcriptomes of CFs obtained from RCM patients and healthy CFs were analyzed using integrated differential expression and pathway analysis (iDEP).[24]

Statistical Analysis

All data are expressed as means±standard error. All statistical analyses were performed using EZR software (http://www.jichi.ac.jp/saitama-sct/SaitamaHP.files/statmedEN.html).[25] Statistical comparisons were performed by using a Student's t-test or Mann-Whitney U-test. A P value <0.05 was considered to indicate statistical significance.

Results

Patient Profiles and Establishment of CFs

The clinical characteristics of all patients are summarized in the **Table** and **Figure 1**. All patients were diagnosed with idiopathic RCM between the ages of 8 months to 7 years. Secondary RCM including cardiac amyloidosis, sarcoidosis, congenital metabolic disorders, or pericarditis were ruled out by cardiac biopsy, echocardiography, electrocardiography, magnetic resonance imaging, serum amino acid analysis, etc.[26] Heart tissues were harvested during VAD implantation or heart transplantation. The fibrosis ratio calculated by Masson trichrome stain was not significantly different among the patients. Purity of CFs was evaluated by immunocytochemistry (**Supplementary Figure 1**). Cardiomyocytes were excluded during the passage because they failed to proliferate. The healthy CFs were commercially obtained and cultured similarly to CFs from RCM patients. The purity was verified by CD90 staining.

Identification of Gene Mutations Associated With RCM by Whole Exome Sequencing

To investigate whether these RCM patients possess known

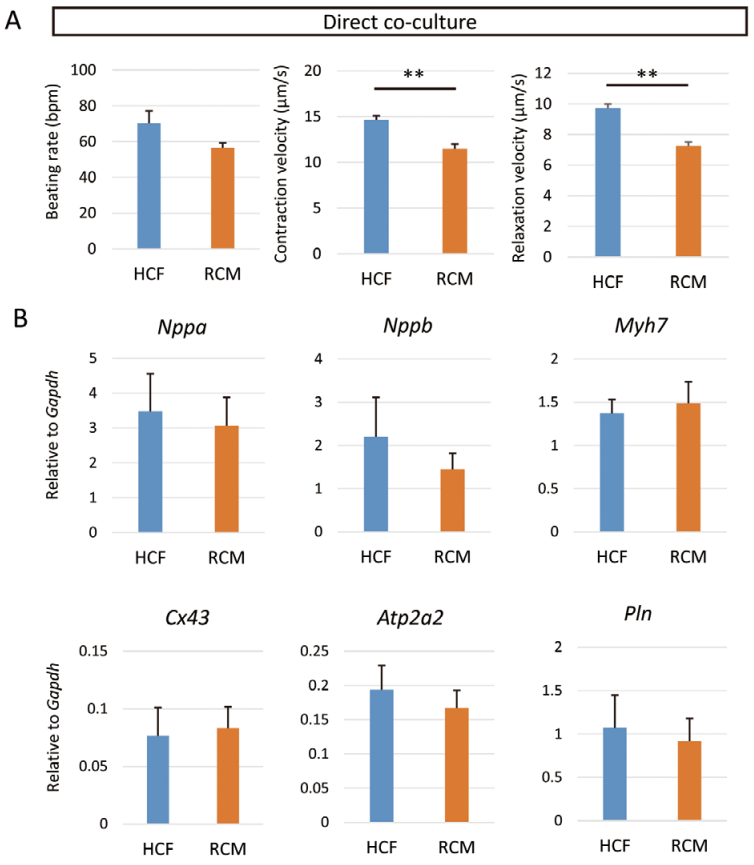

Figure 4. Direct co-culture assays of patient-derived cardiac fibroblasts (CFs) and healthy rat cardiomyocytes. Three independent co-culture experiments were conducted for each patient. Thirty to fifty beating cells were assayed in 1 experiment. The mean values were calculated from 3 different lines of healthy CFs (HCF) and 4 different restrictive cardiomyopathy (RCM) patient-derived CFs. The graphs show mean±standard error. (**A**) Motion analysis under direct co-culture conditions. (**P<0.01). (**B**) Quantitative real-time polymerase chain reaction (PCR) analyses of cardiomyocytes directly co-cultured with CFs by using rat-specific primers.

causative gene variants, we performed whole exome sequencing using peripheral blood samples. We identified the *TNNI3* mutation, more specifically a missense mutation linked to RCM, in 3 of the 4 RCM patients (RCM_1: K178E; RCM_2: R170W; RCM_3: R192H).[6,27] In the other patient (RCM_4), we could not find any candidate variants using this method.[28]

Physiological Features of Cardiac Fibroblasts From RCM Patients

To evaluate general physiological features of CFs from RCM patients, we assessed the ability of proliferation, apoptosis, migration, attachment, and activation toward myofibroblast phenotype. First, we analyzed the ratio of EdU-positive cells for 24 h to assess proliferative ability. We evidenced no significant difference between healthy CFs and those from RCM patients (0.39±0.09 vs. 0.44±0.07, P=0.43; **Figure 2A**). Thereafter, we performed the wound healing assay to investigate the migration capacity of CFs. The shortening of wound distance 12 h after scratching demonstrated no significant difference between healthy CFs and those from RCM patients (0.28±0.15 vs. 0.36±0.12, P=0.51; **Figure 2B**). Additionally, we conducted the cell attachment assay, which indicated no significant difference in the number of adherent cells (251.7±78.3 cells/mm^2 vs. 225.9±47.1 cells/mm^2, P=0.65; **Figure 2C**). Moreover, we investigated the apoptosis of CFs under 4 experimental conditions, more specifically with and without hypoxia and serum deprivation, and evidenced no significant change in CFs from RCM patients (**Figure 2D**). We also counted the number of α-smooth muscle actin (α-SMA)-positive CFs to identify activated fibroblasts, known as myofibroblasts.[29] In our experiment, neither hypoxia nor serum deprivation increased the amount of α-SMA-positive cells (**Figure 2E**). Collectively, we could not identify any significant differences between healthy CFs and those of RCM patients regarding basic cellular behaviors. Additionally, no individual differences were identified among each sample, regardless of disease and *TNNI3* mutations (**Supplementary Figure 2**).

Diastolic Function of Healthy Cardiomyocytes Was Impaired by Co-Culture With CFs From RCM Patients

To investigate whether CFs from RCM patients could affect the motional behavior of cardiomyocytes through paracrine effects or direct cell-cell contact, we performed both indirect and direct co-culture assays with neonatal rat cardiomyocytes. We evaluated the motion vectors of beating cardiomyocytes after 48 h co-culture with heathy CFs and those from RCM patients using a Sony SI8000 motion analyzer (**Supplementary Figure 3**).

The indirect co-culture experiment evidenced that the beating rate and contraction velocity of cardiomyocytes co-cultured with CFs from RCM patients was not significantly different (66.9±18.6 beats/min vs. 72.0±14.9 beats/min, P=0.48 and 10.4±1.62 μm/s vs. 9.2±0.81 μm/s, P=0.21, respectively). Interestingly, the relaxation velocity of cardiomyocytes co-cultured with CFs from RCM patients

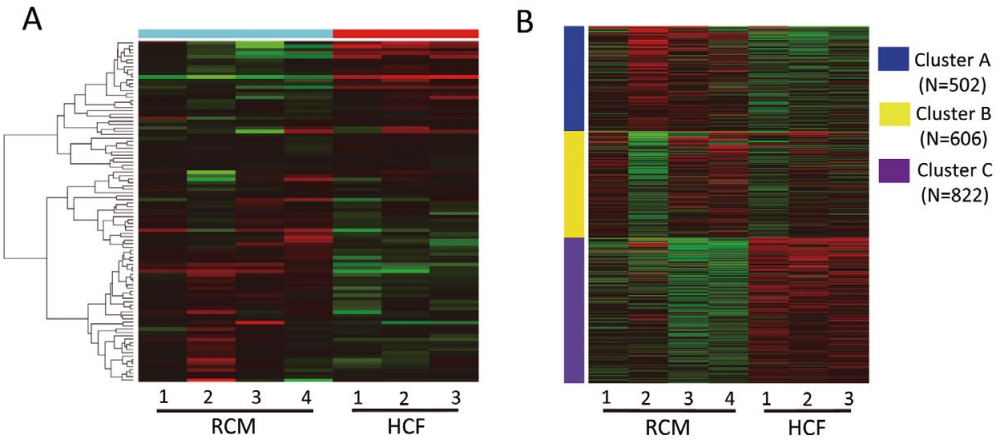

C

Cluster A

adj.Pval	nGenes	Pathways
9.5e-23	151	Anatomical structure morphogenesis
3.2e-20	176	Animal organ development
5.5e-19	81	Circulatory system development
5.8e-18	97	Cell adhesion
5.8e-18	97	Biological adhesion
5.8e-18	189	Cell differentiation
5.8e-18	195	Cellular developmental process
4.1e-17	117	Tissue development
4.6e-16	79	Cellular component morphogenesis
2.5e-15	132	Regulation of developmental process
1.1e-14	76	Anatomical structure formation involved in morphogenesis
1.6e-14	110	Movement of cell or subcellular component
3.2e-14	120	Nervous system development
2.3e-13	100	Locomotion
2.4e-13	110	Cell development

Cluster B

adj.Pval	nGenes	Pathways
7.9e-17	145	Anatomical structure morphogenesis
5.2e-13	154	Regulation of multicellular organismal process
2.9e-12	41	Extracellular matrix organization
3.8e-12	71	Tube development
1.9e-11	43	Extracellular structure organization
6.2e-11	85	Cell migration
1.4e-10	106	Movement of cell or subcellular component
1.7e-10	59	Tube morphogenesis
2.3e-10	89	Cell motility
3.2e-10	84	Cell adhesion
3.4e-10	97	Locomotion
6.0e-10	66	Circulatory system development
6.7e-10	79	Positive regulation of developmental process

Cluster C

adj.Pval	nGenes	Pathways
3.9e-34	191	Cell proliferation
6.6e-31	243	Regulation of multicellular organismal process
1.3e-26	115	Tube development
2.4e-26	140	Cell migration
2.3e-25	171	Movement of cell or subcellular component
4.7e-25	161	Cell cycle
4.8e-25	103	Mitotic cell cycle process
4.8e-25	201	Anatomical structure morphogenesis
1.6e-24	111	Mitotic cell cycle
2.4e-24	157	Locomotion
2.4e-24	144	Cell motility
2.4e-24	111	Circulatory system development
5.9e-24	97	Tube morphogenesis
5.3e-23	55	Mitotic nuclear division

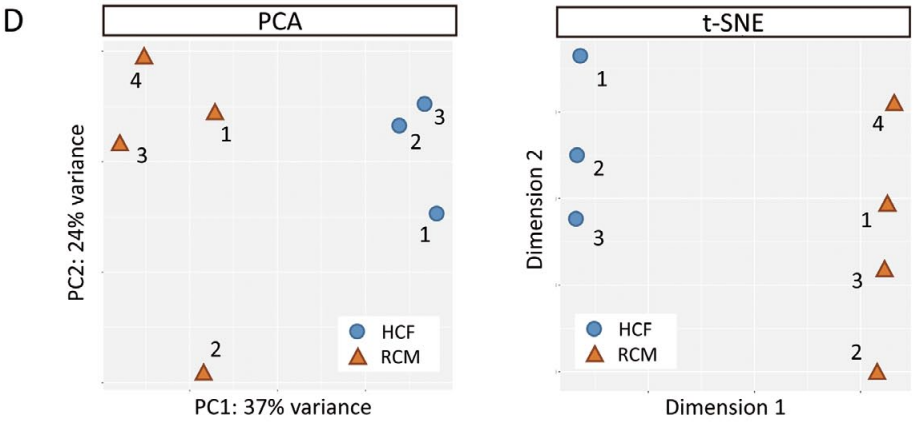

Figure 5. RNA-Seq analyses for cardiac fibroblasts (CFs) derived from restrictive cardiomyopathy (RCM) patients. (**A**) Hierarchical clustering of RNA-seq in healthy CFs (HCF) and RCM CFs. (**B**) K-means clustering analysis of the top 2,000 differentially expressed genes. (**C**) Enriched pathways in each cluster revealed by gene ontology (GO)-term analyses. (**D**) Principal component analysis (PCA; **Left panel**) and t-distributed Stochastic Neighbor Embedding (t-SNE; **Right panel**) analysis of RNA-seq. Each number represents each RCM patient and healthy control.

was significantly lower than that for healthy CFs (6.7±0.54 μm/s vs. 5.6±0.68 μm/s, P=0.038; **Figure 3A**). We investigated mRNA, including *Myh7*, *Nppa*, *Nppb*, *Cx43*, *Atp2a2*, and *Pln* expression levels of cardiomyocytes; however, no significant differences were detected between healthy controls and RCM patients (**Figure 3B**).

Conversely, both the contraction and relaxation velocity of cardiomyocytes directly co-cultured with CFs from RCM patients were significantly lower than that of healthy CFs (14.7±0.85 μm/s vs. 11.6±1.18 μm/s, P<0.01; 9.7±0.55 μm/s vs. 7.3±0.53 μm/s, P<0.01, respectively; **Figure 4A**), though the beating rate of cardiomyocytes was not significantly changed (70.2±13.9 beats/min vs. 56.7±5.6 beats/min, P=0.12; **Figure 4A**). Additionally, there was no significant differences among each patient regardless of *TNNI3* mutations (**Supplementary Figure 4**). Quantitative polymerase chain reaction (qPCR) did not yield any significant changes (**Figure 4B**). Therefore, CFs from RCM patients affected both the contractile and diastolic behavior of healthy cardiomyocytes via paracrine effects and direct interactions.

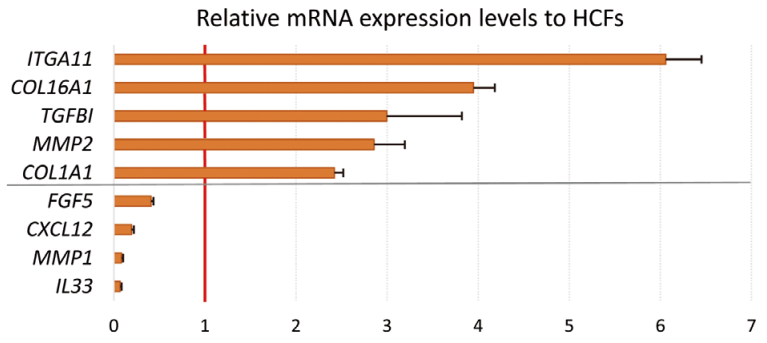

Figure 6. Relative mRNA expression levels in restrictive cardiomyopathy (RCM) cardiac fibroblasts (CFs) obtained by RNA-seq analysis. Differential gene expression analysis demonstrated that *ITGA11*, *COL16A1*, *TGFB1*, *MMP2*, and *COL1A1* were significantly elevated in RCM CFs as compared to healthy CFs. In contrast, *FGF5*, *CXCL12*, *MMP1*, and *IL33* were significantly downregulated in RCM CFs.

Comprehensive Gene Expression Profiling Revealed Distinct mRNA Expression Patterns in CFs From RCM Patients

To investigate expression profiles of CFs from RCM patients, we conducted RNA-seq. Heat map analysis of the top 100 genes demonstrated the different pattern between healthy CFs and those of RCM patients (**Figure 5A**). K-means clustering, dividing the top 2,000 genes into 3 groups, also evidenced similar expression patterns and that the pathways of cell adhesion, cell and tissue development, and extracellular matrix organization were enriched (**Figure 5B**,**C**; **Supplementary CSV File**). Both principal component analysis (PCA) and t-distributed Stochastic Neighbor Embedding (t-SNE) analysis markedly indicated the distinct grouping of healthy CFs and those of RCM patients. However, there was no obvious differences between RCM patients with and without *TNNI3* mutations (**Figure 5D**). This finding indicates that the genetic background of cardiomyocytes did not affect the gene expression patterns of CFs in RCM patients.

Expression of Several Specific Cytokines and Extracellular Matrix Components Were Altered in CFs From RCM Patients

Using the DESeq2 package, with a threshold false discovery rate <0.1 and fold-change >2, we identified 610 upregulated and 649 downregulated genes in CFs from RCM patients. Gene ontology (GO) term enrichment analysis illustrated that genes associated with cytokines and the extracellular matrix were upregulated or downregulated in CFs from RCM patients. The expression of *ITGA11*, *COL16A1*, *TGFBI*, *MMP2*, and *COL1A1* were upregulated in CFs from RCM patients. Reports have evidenced that these factors are elevated in various cardiac disease models.[30–33] In contrast, the expression of *FGF5*, *CXCL12*, *MMP1*, and *IL33* were downregulated in CFs from RCM patients (**Figure 6**). These factors have been reported as protective components for cardiomyocyte homeostasis.[30,34–36] These results indicate that alterations in extracellular matrix composition and humoral factor secretion in RCM CFs might have multiple associations with the impaired contraction and relaxation ability of cardiomyocytes.

Discussion

RCM in children is very rare, but prognosis is extremely poor.[1] As there is no effective therapy for ventricular diastolic dysfunction, elucidation of molecular mechanisms underlying the pathogenesis of RCM it is strongly required. Recently, whole exome sequencing revealed several single nucleotide variants, especially in *TNNI3*, as candidates for causing RCM.[3,4] However, the majority of RCM patients do not possess any candidate variants of cardiomyocyte expressing genes. Moreover, genotype-phenotype correlation is ambiguous in RCM, as well as in other cardiomyopathies.[4,9] These previous findings suggest that we should consider "non-myocyte" factors in the pathogenesis of cardiomyopathy. It is well known that CFs are the most common cell population in the heart. Recently, various studies have demonstrated that CFs play important roles in maintaining cardiac function in ischemic and pressure overload models.[11–13] However, the functions and behaviors of CFs in cardiomyopathy have not been elucidated until now.

In this study, we demonstrated that CFs obtained from pediatric RCM patients exhibited distinct gene expression patterns and deteriorated the relaxation ability of normal cardiomyocytes via paracrine effects and direct cell-cell interaction. To our knowledge, this is the first report that evidences that the cellular character of CFs is altered in cardiomyopathy patients. Moreover, these expression changes were not different among each patient, regardless of *TNNI3* mutation. We identified 3 types of *TNNI3* gene mutation in 4 patients. All of these mutants were reported to increase Ca^{2+} sensitivity of the actin myosin interaction, which might to lead relaxation disability in cardiomyocytes.[27,37,38] As the physiological properties and gene expression patterns of CFs were not significantly different among the RCM patients, regardless of *TNNI3* mutations, we speculated that these properties of CFs from RCM patients were not attributed to genomic disorders of cardiomyocytes or CFs themselves, but to pathological hemodynamic situations or cardiomyocyte-fibroblast interactions in RCM patients in vivo. Additionally, we assume that those features of CFs were maintained in primary culture in vitro. However, we could not clarify how and which specific signals and molecules could affect the expression pattern and characteristics of CFs in RCM patients. Several previous reports have demonstrated that CFs function as a substrate and play important roles in homeostasis in the heart. Furthermore, dysregulation of extracellular matrix components and cytokines has been reported in pathological situations. Our results, obtained from RNA-seq, were consistent with these previous reports evidencing that the expression of *ITGA11*, *COL16A1*, *TGFBI*, *MMP2*, and *COL1A1* significantly increased, whereas *FGF5*,

CXCL12, *MMP1*, and *IL33* were significantly downregulated. The former group of genes were highly expressed in various disease models, whereas the latter listed genes have anti-fibrotic or protective effects on ischemic heart or hypertensive diseases.[30–36] Among them, *TGFB1*, *FGF5*, *CXCL12*, and *IL33* encode secreted proteins, which would be important candidates because our indirect co-culture assay showed significant impairment of diastolic function of cardiomyocytes. TGF β signaling was reported to be associated with cardiac fibrosis and fibroblast activation in the ischemic models; however, we could not reveal any significant difference in the activation of CFs (**Figure 2E**).[31] FGF5 was reported to induce angiogenesis in an ischemic heart model; however, we could not fully elucidated the roles of FGF5 in diastolic dysfunction of cardiomyocytes in this study.[34] CXCL12 and its receptor, CXCR4, were reported to play important roles in embryonic heart development, as well as the maintenance of cardiac functions after birth.[35] Cardiac-specific CXCR4 knock-out mice showed severe systolic and diastolic dysfunction, which lead to death by 13-months of age. Therefore, a decrease of CXCL12 secretion from RCM CFs might cause the cardiomyocyte dysfunction in our co-culture model. IL-33, a family member of IL-1, was reported to play a resistant role for a ischemia and reperfusion model via regulating anti-inflammatory responses and cardiomyocyte apoptosis.[36] Although all or some of these factors might be associated with diastolic dysfunction in co-cultured cardiomyocytes, we could not determine the entire roles that these genes play in the pathogenesis of RCM in our study. Moreover, we assayed the rat cardiomyocytes not the human cardiomyocytes in this study. It is possible that species difference might be a limitation of this study. Further studies are required to identify the specific molecules derived from RCM CFs in regulating human cardiomyocyte diastolic function, though multiple factors might be complexly involved. In contrast, we should note that CFs are not a pure cell population, but rather a heterogeneous population. In this study, we could not determine whether all CFs were altered in RCM patients or only specific subpopulations were affected. Further studies are required to identify critical subpopulations of CFs in RCM. Additionally, we believe that modulating the function of CFs could become a novel therapeutic target for RCM and other cardiomyopathies.

In conclusion, RCM patient-derived CFs demonstrate expression patterns distinct from those of healthy CFs and play important roles in the pathogenesis of RCM by affecting the relaxation ability of cardiomyocytes.

Sources of Funding

This work was supported by grants from the Ministry of Education, Science, Sports, and Culture of Japan [no. 18K07789 and 19K17561].

Disclosures

The authors declare no conflicts of interest.

IRB Information

This research project (no. 15211), as well as the whole exome sequencing using peripheral blood (no. 442), was approved by the Osaka University Clinical Research Review Committee.

Author Contributions

H.T., H.S., and R.W. performed the cellular experiments. H.I., S.K., Y.S., and K.O. managed all experiments, and J.N., R.I., M.T., and T.U. collected and cultured the samples. Y.M., H.K., and Y.A. conducted whole exome sequencing and analysis. H.T. and Y.I. performed RNA-seq analysis. H.T. and H.I. wrote the manuscript and all authors revised and approved the final version of the manuscript.

References

1. Webber SA, Lipshultz SE, Sleeper LA, Lu M, Wilkinson JD, Addonizio LJ, et al. Outcomes of restrictive cardiomyopathy in childhood and the influence of phenotype: A report from the Pediatric Cardiomyopathy Registry. *Circulation* 2012; **126:** 1237–1244.
2. Anderson HN, Cetta F, Driscoll DJ, Olson TM, Ackerman MJ, Johnson JN. Idiopathic restrictive cardiomyopathy in children and young adults. *Am J Cardiol* 2018; **121:** 1266–1270.
3. Kostareva A, Kiselev A, Gudkova A, Frishman G, Ruepp A, Frishman D, et al. Genetic spectrum of idiopathic restrictive cardiomyopathy uncovered by next-generation sequencing. *PLoS One* 2016; **11:** e0163362.
4. Tariq M, Ware SM. Importance of genetic evaluation and testing in pediatric cardiomyopathy. *World J Cardiol* 2014; **6:** 1156–1165.
5. Mogensen J, Kubo T, Duque M, Uribe W, Shaw A, Murphy R, et al. Idiopathic restrictive cardiomyopathy is part of the clinical expression of cardiac troponin I mutations. *J Clin Invest* 2003; **111:** 209–216.
6. Parvatiyar MS, Pinto JR, Dweck D, Potter JD. Cardiac troponin mutations and restrictive cardiomyopathy. *J Biomed Biotechnol* 2010; **2010:** 350706.
7. Wen Y, Xu Y, Wang Y, Pinto JR, Potter JD, Kerrick WG. Functional effects of a restrictive-cardiomyopathy-linked cardiac troponin I mutation (R145W) in transgenic mice. *J Mol Biol* 2009; **392:** 1158–1167.
8. Pinto JR, Parvatiyar MS, Jones MA, Liang J, Potter JD. A troponin T mutation that causes infantile restrictive cardiomyopathy increases Ca2+ sensitivity of force development and impairs the inhibitory properties of troponin. *J Biol Chem* 2008; **283:** 2156–2166.
9. Lee TM, Hsu DT, Kantor P, Towbin JA, Ware SM, Colan SD, et al. Pediatric Cardiomyopathies. *Circ Res* 2017; **121:** 855–873.
10. Mogensen J, Hey T, Lambrecht S. A systematic review of phenotypic features associated with cardiac troponin I mutations in hereditary cardiomyopathies. *Can J Cardiol* 2015; **31:** 1377–1385.
11. Kakkar R, Lee RT. Intramyocardial fibroblast myocyte communication. *Circ Res* 2010; **106:** 47–57.
12. Deb A, Ubil E. Cardiac fibroblast in development and wound healing. *J Mol Cell Cardiol* 2014; **70:** 47–55.
13. Doppler SA, Carvalho C, Lahm H, Deutsch MA, Dressen M, Puluca N, et al. Cardiac fibroblasts: More than mechanical support. *J Thorac Dis* 2017; **9:** S36–S51.
14. Shibamoto M, Higo T, Naito AT, Nakagawa A, Sumida T, Okada K, et al. Activation of DNA damage response and cellular senescence in cardiac fibroblasts limit cardiac fibrosis after myocardial infarction. *Int Heart J* 2019; **60:** 944–957.
15. Justus CR, Leffler N, Ruiz Echevarria M, Yang LV. In vitro cell migration and invasion assays. *J Vis Exp* 2014; **88:** 51046.
16. Beeres SL, Atsma DE, van der Laarse A, Pijnappels DA, van Tuyn J, Fibbe WE, et al. Human adult bone marrow mesenchymal stem cells repair experimental conduction block in rat cardiomyocyte cultures. *J Am Coll Cardiol* 2005; **46:** 1943–1952.
17. Simpson P, Savion S. Differentiation of rat myocytes in single cell cultures with and without proliferating nonmyocardial cells. Cross-striations, ultrastructure, and chronotropic response to isoproterenol. *Circ Res* 1982; **50:** 101–116.
18. Stenzig J, Schneeberger Y, Loser A, Peters BS, Schaefer A, Zhao RR, et al. Pharmacological inhibition of DNA methylation attenuates pressure overload-induced cardiac hypertrophy in rats. *J Mol Cell Cardiol* 2018; **120:** 53–63.
19. Salameh A, Djilali H, Blanke K, Gonzalez Casanova J, von Salisch S, Savtschenko A, et al. Cardiac fibroblasts inhibit beta-adrenoceptor-dependent connexin43 expression in neonatal rat cardiomyocytes. *Naunyn Schmiedebergs Arch Pharmacol* 2013; **386:** 421–433.
20. Chen R, Ge T, Jiang W, Huo J, Chang Q, Geng J, et al. Identification of biomarkers correlated with hypertrophic cardiomyopathy with co-expression analysis. *J Cell Physiol* 2019; **234:** 21999–22008.
21. Salameh A, Wustmann A, Karl S, Blanke K, Apel D, Rojas Gomez D, et al. Cyclic mechanical stretch induces cardiomyocyte orientation and polarization of the gap junction protein connexin43. *Circ Res* 2010; **106:** 1592–1602.
22. Ito M, Hara H, Takeda N, Naito AT, Nomura S, Kondo M, et al. Characterization of a small molecule that promotes cell cycle

activation of human induced pluripotent stem cell-derived cardiomyocytes. *J Mol Cell Cardiol* 2019; **128:** 90–95.
23. Isobe T, Honda M, Komatsu R, Tabo M. Conduction and contraction properties of human iPS cell-derived cardiomyocytes: Analysis by motion field imaging compared with the guinea-pig isolated heart model. *J Toxicol Sci* 2018; **43:** 493–506.
24. Ge SX, Son EW, Yao R. iDEP: An integrated web application for differential expression and pathway analysis of RNA-Seq data. *BMC Bioinformatics* 2018; **19:** 534.
25. Kanda Y. Investigation of the freely available easy-to-use software 'EZR' for medical statistics. *Bone Marrow Transplant* 2013; **48:** 452–458.
26. Muchtar E, Blauwet LA, Gertz MA. Restrictive cardiomyopathy: Genetics, pathogenesis, clinical manifestations, diagnosis, and therapy. *Circ Res* 2017; **121:** 819–837.
27. Cimiotti D, Fujita Becker S, Mohner D, Smolina N, Budde H, Wies A, et al. Infantile restrictive cardiomyopathy: cTnI-R170G/W impair the interplay of sarcomeric proteins and the integrity of thin filaments. *PLoS One* 2020; **15:** e0229227.
28. Tobita T, Nomura S, Fujita T, Morita H, Asano Y, Onoue K, et al. Genetic basis of cardiomyopathy and the genotypes involved in prognosis and left ventricular reverse remodeling. *Sci Rep* 2018; **8:** 1998.
29. Travers JG, Kamal FA, Robbins J, Yutzey KE, Blaxall BC. Cardiac fibrosis: The fibroblast awakens. *Circ Res* 2016; **118:** 1021–1040.
30. Spinale FG. Matrix metalloproteinases: Regulation and dysregulation in the failing heart. *Circ Res* 2002; **90:** 520–530.
31. Khalil H, Kanisicak O, Prasad V, Correll RN, Fu X, Schips T, et al. Fibroblast-specific TGF-beta-Smad2/3 signaling underlies cardiac fibrosis. *J Clin Invest* 2017; **127:** 3770–3783.
32. Talior Volodarsky I, Connelly KA, Arora PD, Gullberg D, McCulloch CA. Alpha11 integrin stimulates myofibroblast differentiation in diabetic cardiomyopathy. *Cardiovasc Res* 2012; **96:** 265–275.
33. Schwanekamp JA, Lorts A, Sargent MA, York AJ, Grimes KM, Fischesser DM, et al. TGFBI functions similar to periostin but is uniquely dispensable during cardiac injury. *PLoS One* 2017; **12:** e0181945.
34. Giordano FJ, Ping P, McKirnan MD, Nozaki S, DeMaria AN, Dillmann WH, et al. Intracoronary gene transfer of fibroblast growth factor-5 increases blood flow and contractile function in an ischemic region of the heart. *Nat Med* 1996; **2:** 534–539.
35. LaRocca TJ, Altman P, Jarrah AA, Gordon R, Wang E, Hadri L, et al. CXCR4 cardiac specific knockout mice develop a progressive cardiomyopathy. *Int J Mol Sci* 2019; **20:** 2267.
36. Ruisong M, Xiaorong H, Gangying H, Chunfeng Y, Changjiang Z, Xuefei L, et al. The protective role of interleukin-33 in myocardial ischemia and reperfusion is associated with decreased HMGB1 expression and up-regulation of the P38 MAPK signaling pathway. *PLoS One* 2015; **10:** e0143064.
37. Yumoto F, Lu QW, Morimoto S, Tanaka H, Kono N, Nagata K, et al. Drastic Ca2+ sensitization of myofilament associated with a small structural change in troponin I in inherited restrictive cardiomyopathy. *Biochem Biophys Res Commun* 2005; **338:** 1519–1526.
38. Gomes AV, Liang J, Potter JD. Mutations in human cardiac troponin I that are associated with restrictive cardiomyopathy affect basal ATPase activity and the calcium sensitivity of force development. *J Biol Chem* 2005; **280:** 30909–30915.

Supplementary Files

Please find supplementary file(s);
http://dx.doi.org/10.1253/circj.CJ-20-1008